Using Mie scattering to determine the wavelength-dependent refractive index of polystyrene beads with changing temperature

Megan R. McGrory,[†,‡] Martin D. King,[‡] and Andrew D. Ward[*,†]

†*STFC, Central Laser Facility, Research Complex at Harwell, Rutherford Appleton Laboratory, Harwell Oxford, Didcot, Oxfordshire, OX11 0FA, UK*

‡*Department of Earth Sciences, Royal Holloway University of London, Egham, Surrey, TW20 0EX, UK*

E-mail: andy.ward@stfc.ac.uk

Abstract

Polystyrene beads are used as test particles in aerosol science. A contact-less technique is reported for determining the refractive index of a solid aerosol particle as a function of wavelength and temperature (20–234 °C) simultaneously. Polystyrene beads with a diameter of 2 µm were optically trapped in air, in the central orifice of a ceramic heating element, and Mie spectroscopy was then used to determine the radius and the refractive index (to precisions of 0.8 nm and 0.0014) of 8 beads as a function of heating and cooling. Refractive index, n, as a function of wavelength, λ (0.480–0.650 µm) and temperature, T, in centigrade, was found to be $n = 1.5753 - (1.7336 \times 10^{-4})T + (9.733 \times 10^{-3})\lambda^{-2}$ in the temperature range $20 < T < 100\,^{\circ}\mathrm{C}$ and $n = 1.5877 - (2.9739 \times 10^{-4})T + (9.733 \times 10^{-3})\lambda^{-2}$ in the temperature range $100 < T < 234\,^{\circ}\mathrm{C}$. The technique represents a step change in measuring the

refractive index of materials across an extended range of temperature and wavelength, in an absolute manner and with a high precision.

Introduction

The real component of the refractive index of a material is important for modelling the light scattering of that materials aerosol.[1] In the atmosphere it is especially critical for evaluation of radiative forcing, for modern climate change.[2] As a material is heated, its volume will change due to thermal expansion and any phase changes, causing a change in the refractive index of that material. There is a need to measure the refractive index of aerosol in the visible spectrum at elevated temperatures for the calculation of light scattering from aerosol produced by processes such as wildfires, [eg 3,4] and biogenic and anthropogenic combustion.[eg 5–8] The intensity of light scattered back to space from aerosol in the Earths atmosphere is a strong function of the aerosol particle's size and refractive index.[1]

Also, an emerging issue in atmospheric science is the transportation and deposition of microplastics, as they may pose serious risks to both human health and the environment.[eg 9–15] It is therefore useful to study the refractive index of one such plastic, polystyrene.

Polystyrene beads are frequently used in atmospheric and aerosol science as a test aerosol particle and for the calibration of instruments such as nephelometers [eg, 16–19] and cavity ring-down aerosol spectrometers. [eg 20–22] Precise measurement of the temperature dependence of the refractive index of polystyrene beads is required for an accurate calibration of such instruments. Miles *et al.*[23] reported that uncertainties in the size and real refractive index of the polystyrene beads, used for calibration of aerosol cavity ring down spectroscopy, lead to errors of up to 2.9% in the measurements of refractive index, demonstrating the need for accurate determinations of the refractive index of polystyrene beads. The uncertainty highlighted in the work by Miles *et al.*[23] would obviously be larger at elevated temperatures because the temperature dependence of the refractive index of the polystyrene beads used

for calibration is unknown.

More traditional methods of measuring the refractive index of a material, such as ellipsometry[24] and refractometry,[25] have previously been used to determine the refractive index of macroscopic thin films of polystyrene as a function of temperature.[26–28] Ellipsometry uses the difference in polarization between the incident and refracted light from a thin film on a surface. Beaucage *et al.*[26] and Efremov *et al.*[28] used ellipsometry to calculate the refractive index of thin films of polystyrene as a function of temperature. Krause *et al.*[27] used a Bausch and Lomb precision refractometer, which measures the angle at which light is refracted when passed through a thin film of material, to determine the refractive index. These methods are normally used on macroscopic thin films, and for a single wavelength.

In an alternative method He *et al.*[29] used microsphere imaging to calculate the refractive index of several polymer beads as a function of temperature. Illuminating the microspheres while they are submerged in oil gives rise to a dark ring in their image. The refractive index can then be determined from the ratio of the size of the dark ring to the size of the microsphere. The microsphere imaging described by He *et al.*[29] only determines the refractive index at one wavelength of light, and measurements are dependent on the values and ncertainties of the refractive index of the oil used. The temperature dependences of the refractive index of polystyrene reported by Beaucage *et al.*,[26] Efremov *et al.*,[28] He *et al.*[29] and Krause *et al.*[27] do not agree and are limited to single wavelengths. Thus, there is a need for a technique that can report the wavelength-dependent refractive index of polystyrene as a function of temperature. It would be advantageous if the method avoided potential contamination by oils and did not rely on the value and uncertainty of reference refractive index.

Described here, optical trapping was used along with a ceramic toroidal-shaped heater to record the Mie spectra (intensity of backscattered white light as a function of visible wavelength) produced by polystyrene beads of approximately 2 µm diameter, trapped in air, as the temperature was varied between 20 °C and a maximum of 234 °C through a range of

heating and cooling cycles. Measurements were taken across the glass transition temperature, T_g, and up to the melting point of polystyrene. The glass transition temperature, T_g, is the temperature at which a polymer transitions from an equilibrium, liquid-like or rubbery state, into a non-equilibrium glassy state as a result of the restriction of molecular mobility.[30] The glass transition causes significant, additional change in the refractive index of polystyrene. The method described here was used to determine the glass transition temperature of airborne polystyrene particles.

Optical trapping is a powerful technique for studying the Mie scattering of airborne particles.[31–39] Precise measurements of both the radius and the wavelength-resolved refractive index have been obtained to a precision of $\pm 0.8\,\mathrm{nm}$ and 0.0014 respectively, by reproducing experimental Mie spectra of trapped particles with calculated Mie spectra using known values of radius and wavelength-resolved refractive index. Polystyrene was an exemplary material for this study as it has two well-known phase transitions, its glass transition temperature, which has been reported as values between $96.9\,^{\circ}\mathrm{C}$ and $107\,^{\circ}\mathrm{C}$,[40–44] and its melting point $240\,^{\circ}\mathrm{C}$.[40] The phase transition temperatures have been used to validate the experimental variation of refractive index with temperature measurement.

Method

The strategy for performing the experiment was to levitate an airborne, solid, spherical, polystyrene bead, in air, using an optical trap.[32] Throughout this paper the back scattered white light from the trapped particle is referred to as a Mie spectrum. The temperature in the trapping cell was changed in steps, allowing the temperature to equilibrate between the apparatus and the bead at each step. The Mie spectra of back-scattered light was continuously recorded using a spectrometer with a three second integration. These experimental Mie spectra were then reproduced as calculated theoretical spectra from a known refractive index as a function of wavelength, described by a Cauchy equation,[45] and a known radius to

determine the refractive index of the bead as a function of both wavelength and temperature.

Optical trapping of airborne particles

The optical setup of the laser trap is shown in Figure 1, and has been described in detail previously.[32] A 1064 nm Nd:YAG laser (Laser Quantum) was coupled to two single-mode fibre-optic cables via a beam-splitter coupling port (Oz Optics) and used to deliver laser beams of power 10 mW and 15 mW (measured at the point of focus) pointing upwards and downwards respectively. The beams were focused using two Mitutoyo M Plan Apo x50 NA 0.42 objectives into an aluminium trapping cell and aligned to sub-micron accuracy using a 3-axis piezo-electric stage (Physik Instrumente). Polystyrene beads (Invitrogen batch S37500) of reported diameter (2.0 ± 0.1) µm suspended in water were aerosolized using an atomizer (Topas, ATM 220) and delivered as dry beads into the aluminium trapping cell via a diffusion dryer filled with silica gel. The process of trapping involved several beads being delivered into the cell and the position of the cell, containing the aerosol, was adjusted relative to the laser focus until a single bead was trapped at the point of focus. The remaining beads were removed by collisions with the cell walls over a period of approximately 2 minutes.

Heating apparatus

The toroidal-shaped ceramic heater (Thorlabs HT19R) was placed inside the aluminium trapping cell, such that the focus of the counter-propagating laser beams are delivered through the 4 mm aperture in the heater. See Figure 2. The heated volume inside the torus and thus adjacent to where a polystyrene bead was to be held in the optical trap was $\sim 0.5\,\mathrm{cm}^3$.

The ceramic heater was used to control the temperature of the polystyrene bead and surrounding air. A detailed diagram of the heating cell is shown in Figure 2. The top and bottom heater clamps were constructed from Macor. Macor is a low thermal conductivity composite and thus insulates the heating element from the external components of the cell. The temperature of the polystyrene particle was set by the current flowing through the

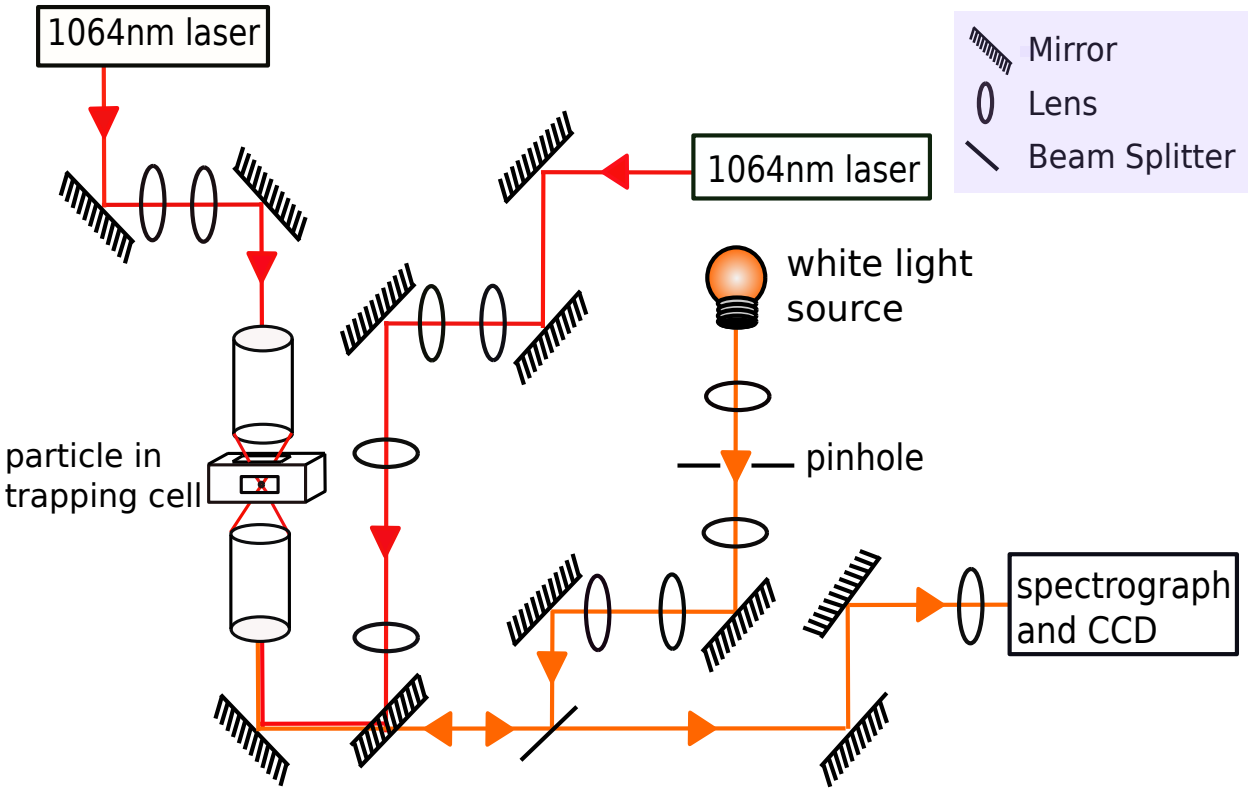

Figure 1: Optical set up of laser trap.

heater. The temperature was calibrated by placing a K-type thermocouple in the centre of the heater instead of the trapped particle. During the experiments with a trapped polystyrene bead, the temperature of the heater was monitored by a K-type thermocouple in contact with the heater. The uncertainty in the temperature of the particle in the trap, was estimated to be $\pm 1\,^{\circ}\mathrm{C}$, based on the calibration technique.

Mie spectroscopy for trapped particles

As depicted in Figure 1, an LED white light source (Comar 01 LP 555, 6V), with a typical white LED spectrum (for example similar to Thorlabs MCWHL6), illuminated the trapped bead from below. Visible light back-scattered from the polystyrene bead was collected over the wavelength range of 480–660 nm, at a resolution of 0.13 nm, and focused into a spectrograph (Acton SP2500i, 300 groove mm^{-1} grating). The collected Mie spectrum was then imaged onto a charge coupled device (CCD) detector (Princeton Instrument Spec 10:400

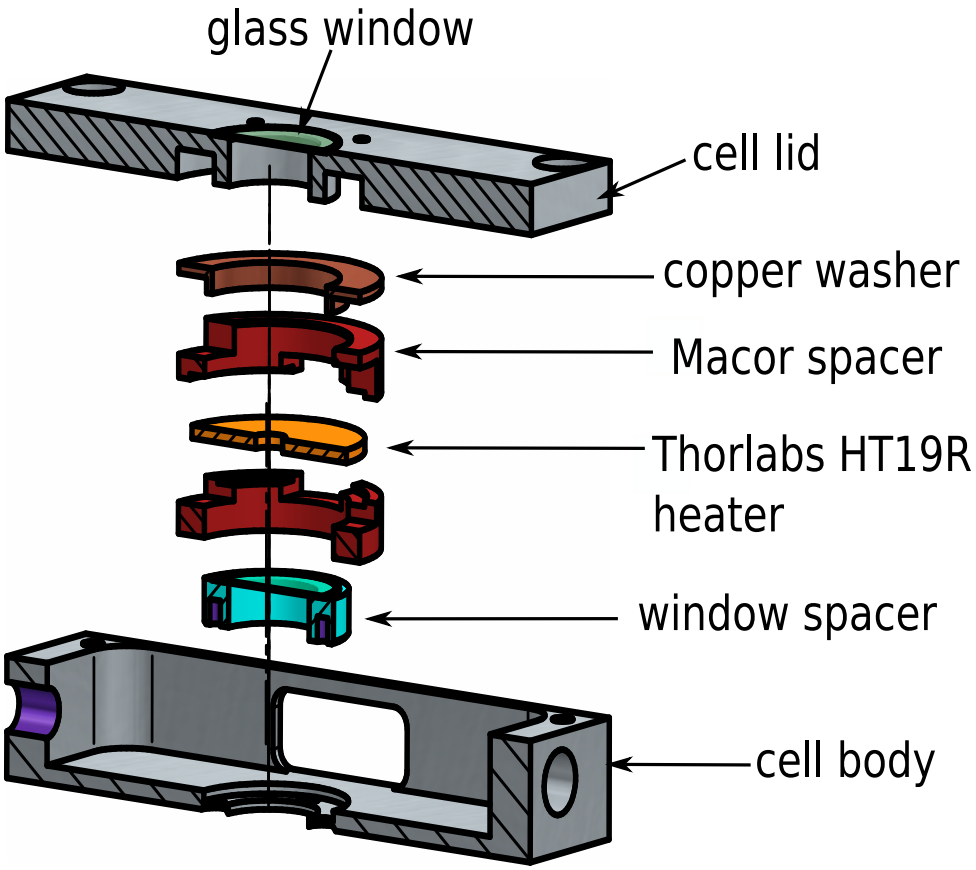

Figure 2: Schematic of the cross section of the aluminium trapping cell demonstrating the positioning of the heater. The long axis of the cell is 7.8 cm and the width is 3.2 cm. The two circular holes on the right hand side of the diagram are for addition and exhaust of aerosol. The counter propagating beams enter from above and below the cell in this orientation.

BR). The wavelength of the spectrograph was calibrated using the gas discharge spectral lines produced by a Hg-Ne PenRay lamp.

Mie spectra were accumulated over three second intervals continuously for each of the polystyrene beads as the temperature was changed. Descriptions of the experiments performed on each bead are summarised in Table 1. The typical rate of heating/cooling of the beads was $\sim 1.8\,^{\circ}\mathrm{C\,min^{-1}}$ for all experiments. For comparison, He *et al.*[29] cooled polystyrene beads at a rate of $10\,^{\circ}\mathrm{C\,min^{-1}}$ and Krause *et al.*[27] cooled polystyrene thin films at a rate of $0.33\,^{\circ}\mathrm{C\,min^{-1}}$ until $10\,^{\circ}\mathrm{C}$ before T_{g}, then at $0.167\,^{\circ}\mathrm{C\,min^{-1}}$ until just before T_{g}, then $0.0017\,^{\circ}\mathrm{C\,min^{-1}}$ in the vicinity of T_{g}.

Table 1: Summary of heating/cooling cycles for all experiments carried out

Bead	Maximum temperature / °C	Heating/Cooling Cycles
PS1	163	Heated, Cooled
PS2	234	Heated up to melting point
PS3	147	Heated, Cooled
PS4	151	Heated, Cooled, Reheated
PS5	180	Heated, Cooled (quickly 3 times)
PS6	180	Heated, Cooled (quickly 3 times)
PS7	180	Heated, Cooled (quickly once)
PS8	175	Heated, Cooled

Data analysis

It is possible to determine the size and wavelength-dependent refractive index of a particle using the Mie spectral peak positions only[32,46–48] or the profile of the Mie spectrum in combination with peak positions.[49,50] Before describing the results, it is useful to explain how the experimental Mie spectra will be modelled to determine the radius, and the wavelength-dependent refractive index. For the work described here, only the peak positions of the Mie spectra were used for determining refractive index and diameter of the particle.

Generating theoretical Mie spectra

The technique described here determines the refractive index, n, as a function of wavelength, λ, using the Cauchy equation,[45]

$$n = A + \frac{B}{\lambda^2} + \frac{C}{\lambda^4}, \tag{1}$$

where A, B and C are material-dependent, empirical constants needed to determine the refractive index as a function of wavelength, λ, of the polystyrene beads. The fitting process is carried out in two steps, named either the 'grid-scan' or the 'Cauchy fitting'.

Firstly, a large parameter space (typically $\sim 10^6$ calculations) for potential values of A, B, C and the radius was searched using a 'grid-scan' method. A second step then refined the best-fit values of A, B, C and the radius produced by the grid-scan. The best-fit values of A,

B, C and radius were found as those that minimised the difference between experimental and calculated peak wavelength positions in the Mie spectra. The fitting process *a priori* assumes the wavelength dispersion of the refractive index was described by a Cauchy equation and that the particle was a sphere.

Step 1: Grid-scan search

In order to determine the radius and the values for the constants A, B and C, from equation 1, and to reproduce the experimentally measured Mie spectra. Theoretical Mie spectra were calculated using the method described by Bohren and Huffman[51] in their Fortran `BHMie` code. A program was written in Python3 based on the `BHMie` method that was modified for calculating the scattering over the numerical aperture of the objective lens at 0.5° intervals to match our experimental data. The program was used to generate a 4-dimensional space of theoretical spectra for a given range of each of the parameters A, B, C and radius, r. A grid search of such a large parameter space allowed for the identification and disregard of false minima.[49] The figure-of-merit for assessing a goodness-of-fit between the calculated and experimental Mie spectra was the average difference between the experimental and calculated peak positions in the wavelength range 480–650 nm. The values of the parameters, A, B, C and r, that describe the theoretical spectrum with the smallest average peak position difference relative to the experimental Mie spectrum, were taken as the starting point for secondary step in the fitting process, 'Cauchy fitting'. The resolution of the 4-dimensional grid-scan search were as follows; A at a precision of 1×10^{-4}, B at a precision of 5×10^{-5} µm^2, C at a precision of 1×10^{-6} µm^4, radius at a precision of 2 nm and wavelength at a precision of 0.05 nm. The 'Cauchy fitting' step was at higher precision, so finer resolution at this stage was unwarranted.

Step 2: Cauchy fitting

For a range of radii (10 nm above and below the 'best radius' found from the grid-scan step, at a precision of 1 nm) each peak in the experimental Mie spectrum was fitted using a peak comparison to the equivalent peak in the theoretical spectrum. ±10 nm was found to be a reasonable range that resulted in finding a clear best-fit, and therefore most probable radius.[52] For each value of radius, the refractive index at each wavelength that corresponded to a peak position, was then plotted as a function of wavelength. A Cauchy curve was then fitted to the refractive indices against wavelength plot using a Levenberg-Marquardt algorithm. A figure of merit, ϕ, was found for each Cauchy curve, by combining the errors of each of the Cauchy parameters, A, B and C, using the equation,

$$\phi = \sqrt{\sum_{i=1}^{N} \Delta A^2 + \frac{\Delta B^2}{\lambda_i^2} + \frac{\Delta C^2}{\lambda_i^4}}, \tag{2}$$

where λ_i is the wavelength of the i^{th} peak and N is the number of peaks in the Mie spectrum. The minimum in the resulting plot of ϕ versus radius, along with the determined values of A, B and C from the fit were taken to be the most probable parameters of the polystyrene bead.

The overall uncertainty for both steps of this fitting process was estimated by carrying out the two step process on an indicative number (10) of spectra fitted per typical experiment. Ten different spectra of the same particle were taken 3 seconds apart and the standard deviation of the radii was determined for the 10 spectra. The standard deviation of the radii was found to be ±0.8 nm, which leads to an average uncertainty in the refractive index of ±0.0014

Thermal expansion coefficient

The aim of this work was to produce a precise determination of the refractive index of polystyrene spheres as a function of temperature. However, the change in radius of the

particle was also measured to a precision of $\pm 0.8\,\mathrm{nm}$. Thus, enabling a calculation of volume changes of the polystyrene bead with heating. The volumetric thermal expansion coefficient of a solid,

$$\alpha_V = \frac{1}{V}\frac{\delta V}{\delta T}, \tag{3}$$

where V is the volume of the solid and T is the temperature (δV is the fractional amount by which the volume will expand when heated by δT). Comparing the volume change as a function of temperature with literature values for polystyrene[40] will validate the calibration of the heating cell.

Results

The results focus on the comparison of experimental Mie spectra with calculated Mie spectra. Comparison of the Mie spectra has enabled the determination of refractive index as a function of wavelength and size. The variation in these parameters with temperature were then reported to demonstrate the thermal expansion and phase change of spherical polystyrene beads.

Mie spectra fitting

Figure 3 shows the change in Mie spectra as a typical bead (PB2) was heated from room temperature, 22 °C to 234 °C. The melting point of polystyrene is 240 °C. The experimental data in Figure 3 are shown by the solid lines and the calculated Mie spectra are shown by the dashed lines. Figure 3 demonstrates the excellent reproduction of the experimental data. The Mie spectra are vertically offset for clarity. The vertical dotted lines track the progression of the Mie spectra peak positions as the temperature rises.

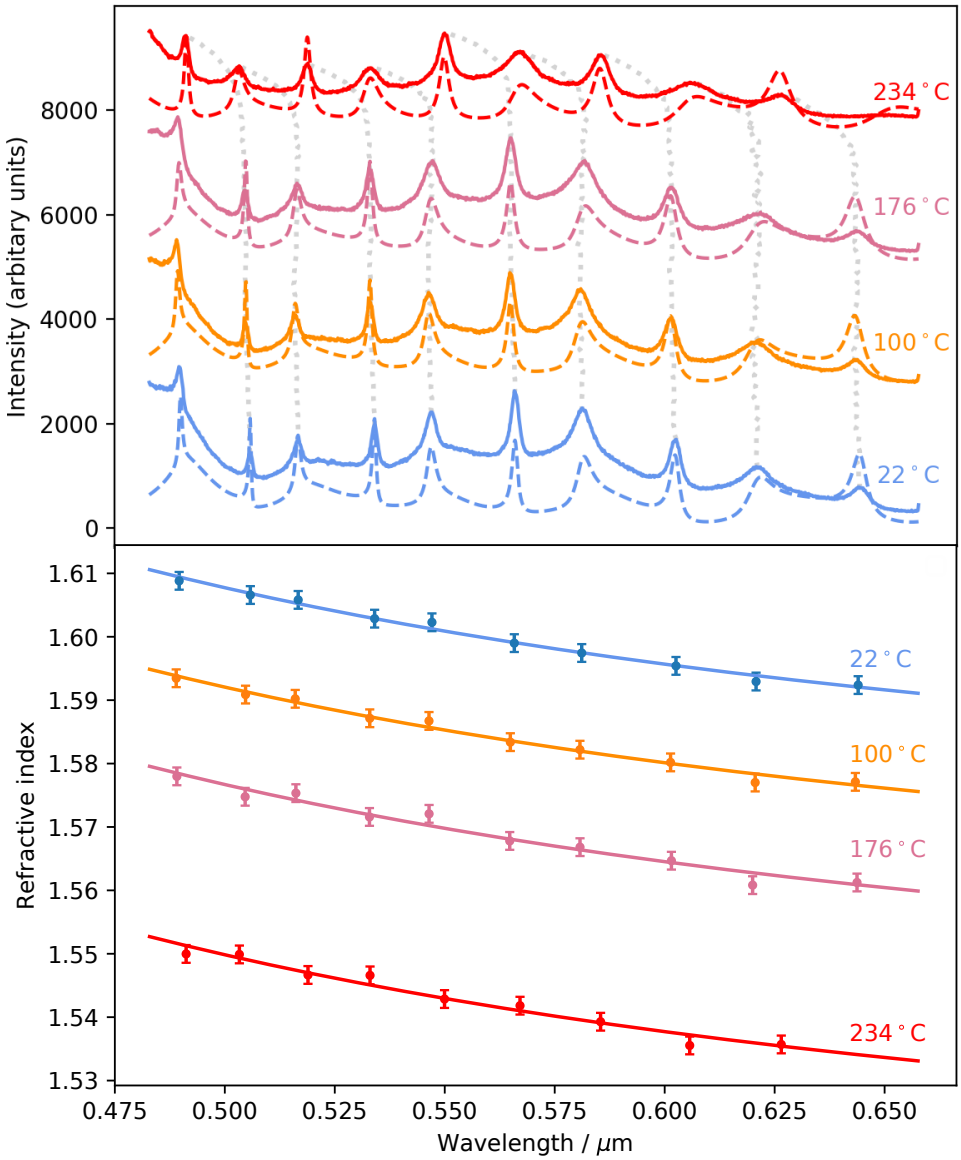

Figure 3: The top panel shows the experimental Mie spectra (solid lines) of polystyrene bead (PB2) in air at 22 °C, 100 °C, 176 °C and 234 °C. Each experimental Mie spectrum is compared with their matching calculated spectra (dashed lines) from Mie theory. The shift in peak positions between 22 °C and 234 °C is also shown as vertical dotted lines. Note that the spectra are shifted vertically, for each temperature, for clarity. The bottom panel shows the refractive index of a polystyrene bead as a function of wavelength for polystyrene bead PB2, at four separate temperatures. The points are plotted at the positions of peaks in the Mie spectrum. Uncertainty in refractive index is ±0.0014.

Refractive index variation as a function of temperature

A total of eight different polystyrene beads were studied, as summarised in Table 1. The refractive index (at a wavelength of 589 nm) for all polystyrene beads studied as a function

of temperature are shown in Figure 4. The real component of the refractive index decreased with an increase in temperature. The rate of change in refractive index with temperature is different before and after the glass transition temperature, (T_g). The rate of change of refractive index with temperature was found to be independent of wavelength. A demonstration of the rate of change of refractive index being independent of wavelength is included in the supplementary information. It is noted that beads from the same sample were polydisperse in both size and refractive index.[32] The range of measured refractive indices for the polystyrene bead sample was broad, from 1.5923 to 1.6009 at room temperature. Thus, the phase change at T_g was calculated from a single bead (PB2) by extrapolation of linear fits between refractive index and temperature between 20 °C and 90 °C, and, 110 °C and 150 °C. The intersection of these linear fits was at a temperature of 100.2 °C which falls into the range of literature values 96.9 °C and 107 °C.[40–44] There was no observation of hysteresis in either radius or refractive index over a cycle of heating and cooling.

The change in the refractive index as a function of temperature, at a wavelength 589 nm, for all beads, is compared with experiments by Krause *et al.*,[27] Beaucage *et al.*[26] and He *et al.*[29] in Figure 4 (inset). It should be noted that the experiments by Beaucage *et al.*[26] and He *et al.*[29] were carried out at wavelengths of 633 nm and 532 nm respectively, while the data plotted in Figure 4 and Krause *et al.*[27] are reported at 589 nm. Figure 3 shows the refractive index of a bead (PB2) as a function of wavelength for a range of temperatures (22–234 °C), which demonstrates that the refractive index can be defined by a Cauchy equation (1) across the temperature range studied.

The wavelength-dependent variation of the refractive index is defined here by the parameters A, B and C of the Cauchy equation (1). Figure 5 shows the values of A, B and C as a function of temperature. The variation in A was found to have statistically significant linear correlation with temperature below and above T_g, described by equations 4 and 5,

$$A = (1.5753 \pm 0.0072) - ((1.7336 \pm 0.0522) \times 10^{-4})T; \qquad 22\,^{\circ}\mathrm{C} < T < 100\,^{\circ}\mathrm{C} \qquad (4)$$

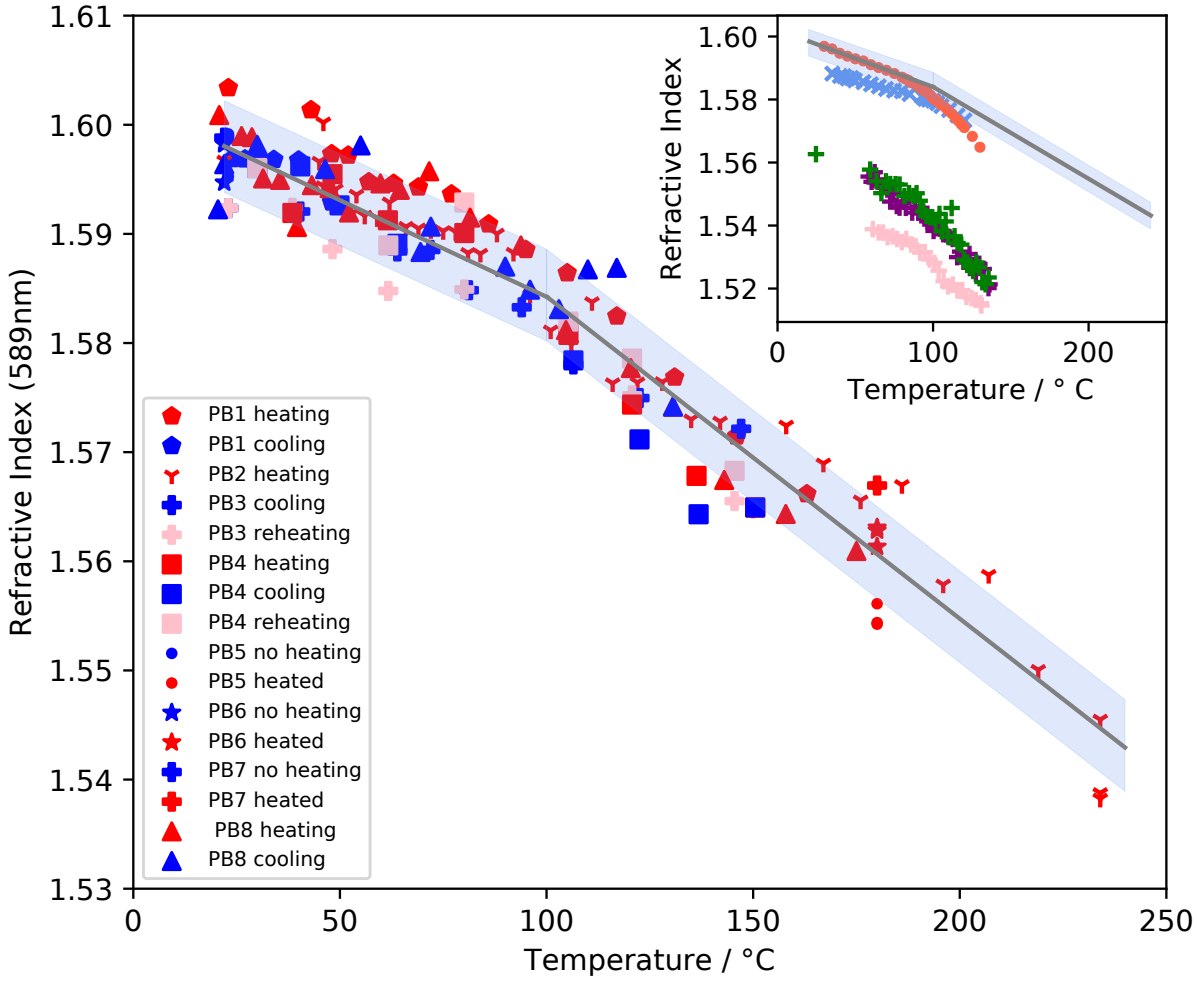

Figure 4: The refractive index at 589 nm for all polystyrene beads as a function of temperature. The grey line is a linear fit, to guide the eye, of the refractive index before and after T_g, determined from bead PB2 as (T = 100.2, n = 1.5842). The shaded area represents 3 standard deviations in refractive index. The inset replots the data, compared with results from He *et al.* (red dots- refractive index reported at 532 nm),[29] Beaucage *et al.* (green, purple and pink '+' symbols- refractive index reported at 633 nm),[26] and Krause *et al.* (blue '×' symbols- refractive index reported at 589 nm).[27]

$$A = (1.5877 \pm 0.0140) - ((2.9739 \pm 0.1345) \times 10^{-4})T; \qquad 100\,^{\circ}\mathrm{C} < T < 234\,^{\circ}\mathrm{C} \qquad (5)$$

below and above T_g respectively. Parameters B and C had no statistically significant correlation with temperature. The value if B is the average value, $9.73 \pm 0.3 \times 10^{-3}\mu m^2$ and C is effectively $0\,\mu m^4$. Thus, the change in refractive index with wavelength is summarised

by the equations;

$$n = (1.5753 \pm 0.0072) - ((1.7336 \pm 0.0522) \times 10^{-4})T + \frac{(9.7333 \pm 0.3001) \times 10^{-3}}{\lambda^2} \quad (6)$$

and

$$n = (1.5877 \pm 0.0140) - ((2.9739 \pm 0.1345) \times 10^{-4})T + \frac{(9.7333 \pm 0.3001) \times 10^{-3}}{\lambda^2} \quad (7)$$

in the temperature ranges 20 °C < T < 100 °C and 100 °C < T < 234 °C respectively.

Thermal expansion of polystyrene beads

The change in bead radius as a function of temperature was determined for all beads. Figure 6 shows the change in radius for bead PB2. All other beads studied exhibited similar behaviour, but because bead size at room temperature for the other polystyrene beads varied between 0.986 µm and 1.007 µm they are not shown for clarity.

Figure 6 shows maximum and minimum theoretical radii calculated from the thermal expansion literature values of α_V, both below and above T_g [40]. Below the glass transition temperature, T_g, the expansion of the bead agrees with literature within literature uncertainty. Above T_g, the expansion of the polystyrene bead agrees with literature within literature uncertainty until 150 °C, after which point there is slight deviation. Approaching 240 °C, the polystyrene bead starts to melt causing the volume to decrease rapidly.

Discussion

Radius and refractive index as a function of temperature

The refractive index of polystyrene is dependent on its chemical and physical properties, following the Lorentz-Lorenz equation, [53]

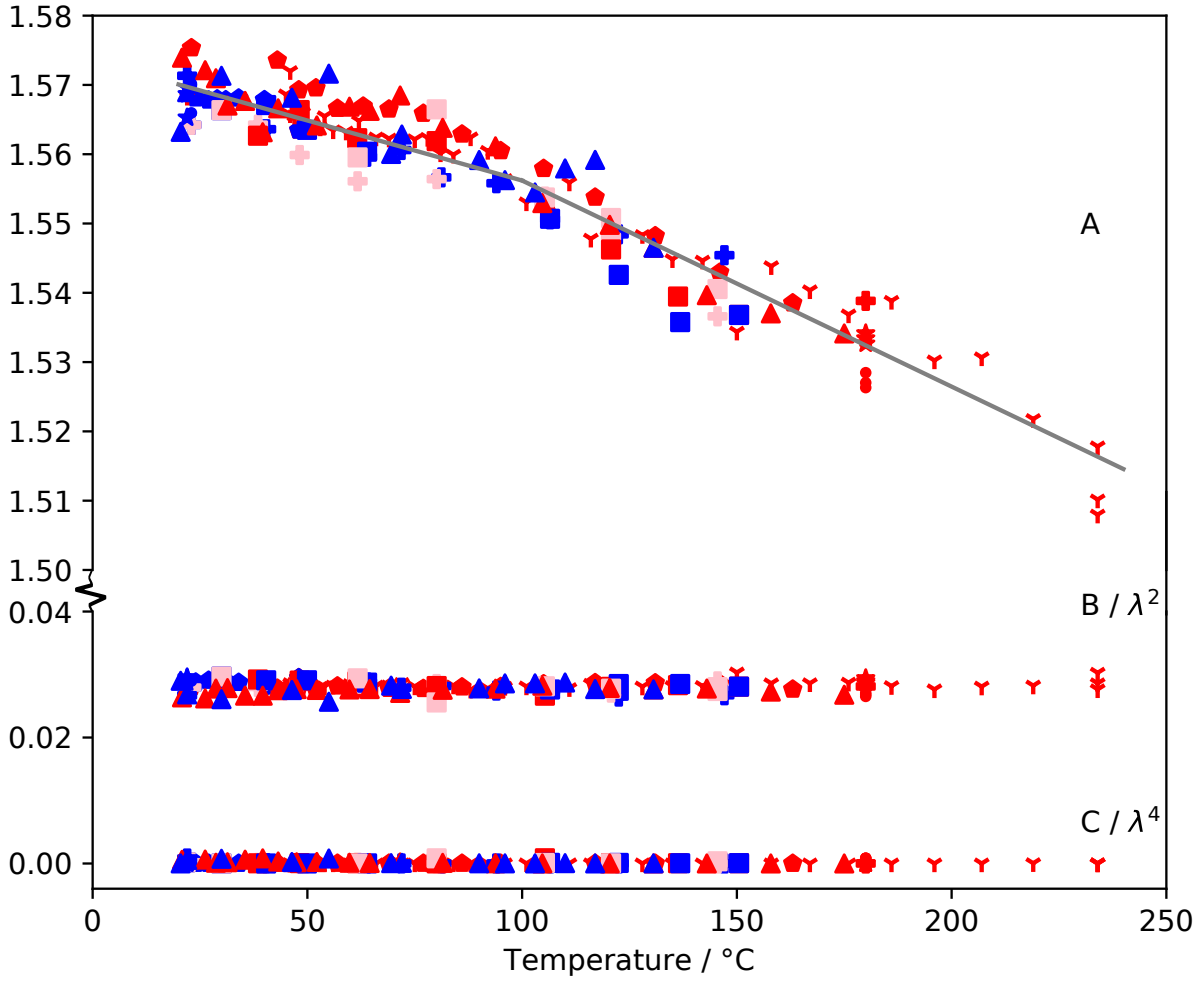

Figure 5: Cauchy equation (1) parameters A, B/λ^2 and C/λ^4, as a function of temperature. The plot demonstrates the contribution of each of the terms in the equation (1) to the change in refractive index as a function of temperature. The legend is the same as the legend from Figure 4.

$$\frac{n^2-1}{n^2+2} = \frac{N\alpha\rho_m}{3M} \tag{8}$$

where n is the refractive index, ρ_m is the mass density, N is Avogadro's constants, α is the mean polarizability and M is the molecular weight of the polystyrene. As N and M are constant, and α is found to be effectively constant with changing temperature,[54] then the density is the significant factor determining the change in refractive index as a function of temperature.[55–57]

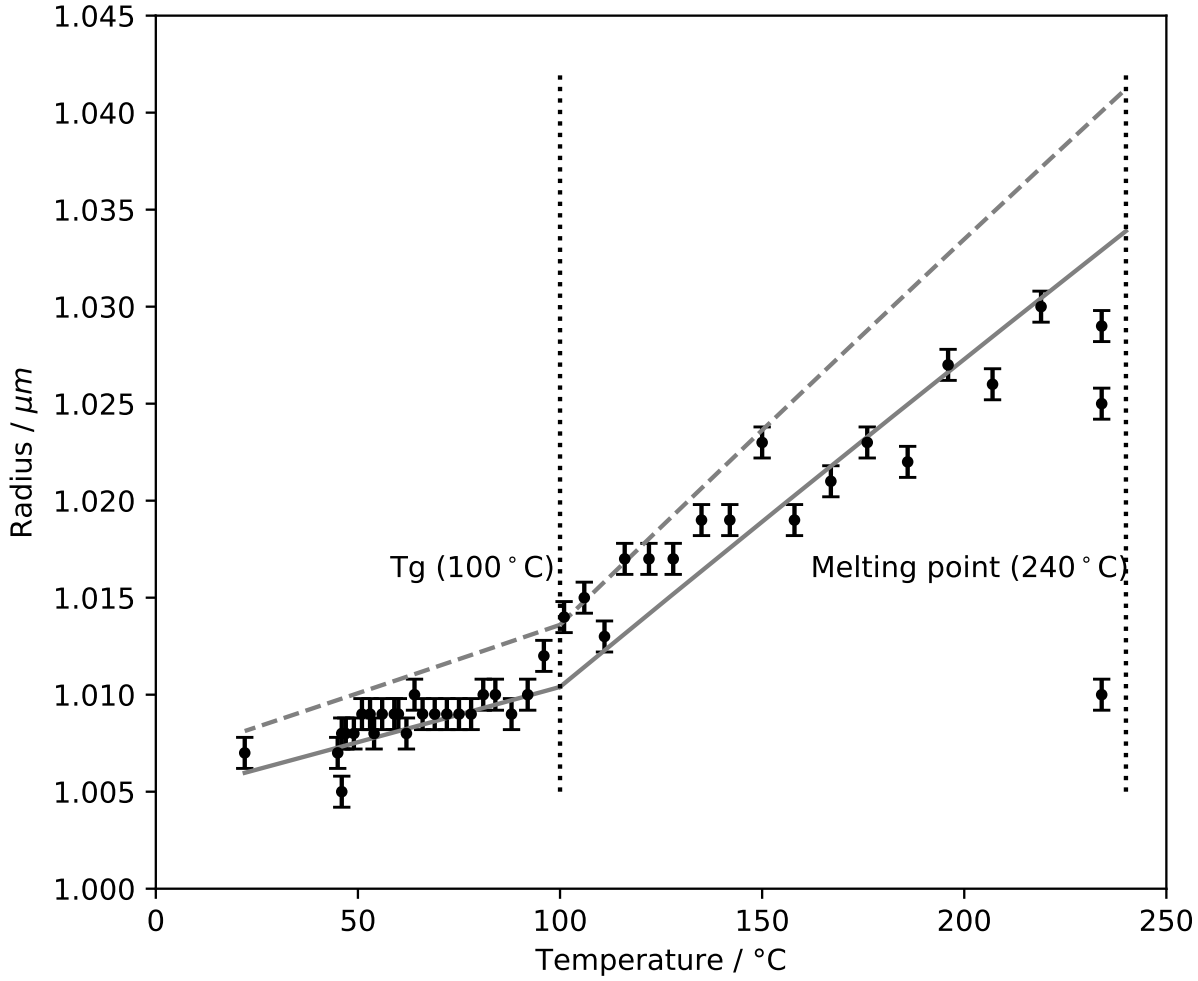

Figure 6: Radius as a function of temperature for polystyrene bead PB2, compared with minimum (solid line) and maximum (dashed line) radii based on literature values for the volumetric thermal expansion coefficient[40]

.

As the polystyrene beads are heated thermal expansion causes the the mass density, ρ_m to decrease, causing a decrease in refractive index. This is consistent with results found in this study, where an increase in radius and a decrease in refractive index was found as the temperature increased, with the rate of change increasing at the glass transition temperature, due to physical changes occurring more rapidly at this point.

Measurements were carried out from room temperature to 234 °C, just below the melting point of polystyrene (240 °C) without disturbing the optical trapping stability. The particle

was stable in the trap throughout the changes. Even approaching the melting temperature the bead was retained for sufficient time to enable spectral acquisitions indicating a rapid loss of material, possibly due to evaporation of monomer and short chain polymer styrene and polystyrene molecules. The wavelength-dependent refractive index determined at room temperature compares well within uncertainty with previous work.[32]

Figure 4 shows a comparison between the determined refractive index of all results obtained with results from He *et al.*,[29] Beaucage *et al.*,[26] and Krause *et al.*,[27] which were all monochromatic studies. The inset in Figure 4 compares the refractive index data recorded by others[26,27,29] at similar, but different, wavelengths. There is good agreement between this study and He *et al.*,[29] before the glass transition temperature (T_g), where Krause *et al.*[27] found the refractive index to be slightly lower and Beaucage *et al.*[26] found the refractive index to be substantially lower. The offset observed between this study and that of Krause *et al.* and Beaucage *et al.* is likely to be due to differences in the properties of the polystyrene studied. The glass transition temperatures for all four studies were: 100.2 °C for this study, 98.3 °C for He *et al.*, 100 °C for Krause *et al.* and 86.4 °C, 91.6 °C and 111.5 °C for Beaucage *et al.* at different film thicknesses.

The polystyrene beads used by He *et al.* were immersed in oil and were approximately 60 µm in diameter, where as here they were only approximately 2 µm in diameter. Both Krause *et al.* and Beaucage *et al.* studied thin films of polystyrene. The heating rate was also different in each of the experiments. In this study the beads were heated and cooled at $\sim$1.8 °C min^{-1}, He *et al.*[29] cooled polystyrene beads at a rate of 10 °C min^{-1}, Krause *et al.*[27] cooled polystyrene thin films at a rate of between 0.33–0.0017 °C min^{-1} and Beaucage *et al.* heated and cooled polystyrene films at a rate of 2 °C min^{-1}.

The recorded thermal expansion of a single polystyrene bead is in agreement with literature values of the thermal expansion of bulk polystyrene at temperatures below 150 °C, as shown in Figure 6. The difference above this temperature, namely, a lower expansion than expected may be due to loss of lower molecular weight material from the bead as it

approaches the melting point. He *et al.*, Krause *et al.* and Beaucage *et al.* all do not exceed 140 °C in their reported measurements.

A limitation of this technique is that only one particle can be studied at a time. However the technique can be used to determine the refractive index over a range of wavelengths between $480 - 650$ nm, rather than for a single wavelength, and the size of the particle at the same time. It would also be possible to determine the change in density with temperature provided the density at room temperature is known. The technique gives an absolute measurement, therefore is not measured relative to the refractive index of another material. As the particles are airborne rather than submerged in oil, it is a contact-less method and the medium (air) will not affect the light scattered by the particle, or have the potential for particle contamination. Air is an excellent choice of bath gas because its refractive index variation with temperature is well documented and is almost unity, within the precision of our experiment. The refractive index of air does change slightly with temperature, it is 1.00027 at room temperature and 1.00021 at 100 °C,[58] it was found that this change in refractive index of the medium led to no significant change in the determined refractive index or size of the particle, within uncertainty and therefore does not need to be considered.

Polystyrene as a test aerosol

Polystyrene has two distinct phase changes in the temperature range studied. These may be used as reference points to accurately calibrate recorded temperatures, polystyrene is an excellent test aerosol for this system. Figure 6 shows that the glass transition temperature was seen to occur at the expected temperature of 100 °C,[40] and there was evidence for a phase transition approaching the melting temperature of 240 °C,[40] which gives confidence in this method.

Conclusion

A technique has been developed with clear applications in combustion aerosol science, heterogeneous catalysis and climate science, for precisely determining the wavelength dispersion of refractive index, as a function of temperature, for trapped airborne particles. By determining the refractive index of polystyrene beads, as a function of wavelength and temperature simultaneously, and the size as a function of temperature, it has been demonstrated that the technique is robust due to polystyrene's known phase changes. A contact-less method has been demonstrated for measuring the refractive index associated with the phase changes of polystyrene. Presence of a contact surface would compromise such measurements. The technique has the potential to be applied to other airborne particles for measuring the refractive index dispersion during liquid to solid, or solid to liquid, phase changes. The glass transition temperature of polystyrene has been reported as 100 °C and the temperature range of the recorded behavior of polystyrene as a function of temperature has been extended by ~ 100 °C using a polychromatic method.

There is potential for an increase in the temperature range that can be studied using this technique. Higher temperatures could be reached through better insulation and improved cell design. Temperatures below room temperature could be reached by cooling the aluminium cell.

The work presented here represents a step change in measuring the refractive index of airborne particles in an absolute manner, with high precision, as a function of both temperature and wavelength. The work also demonstrates a new development in the measurement of the refractive index of airborne particles, as a function of wavelength and temperature, for measuring phase changes.

Supporting Information

Raw data and full set of results are available at DOI: 10.5281/zenodo.3885730

Acknowledgement

The authors thank NERC for funding of grant NE/R012148/1. We are also grateful to STFC for support under grant 18130025, and for access to the laboratories of the Central Laser Facility at the Research Complex at Harwell. We also thank Olivia Ward for assistance in collecting data for bead PB8 during her placement at the Central Laser Facility.

References

(1) Haywood, J. M.; Ramaswamy, V.; Soden, B. J. Tropospheric Aerosol Climate Forcing in Clear-Sky Satellite Observations over the Oceans. *Science* **1999**, *283*, 1299–1303.

(2) IPCC, Climate Change 2013: The Physical Science Basis. Contribution of Working Group I to the Fifth Assessment Report of the Intergovernmental Panel on Climate Change. 2013.

(3) Gyawali, M.; Arnott, W. P.; Lewis, K.; Moosmüller, H. In situ aerosol optics in Reno, NV, USA during and after the summer 2008 California wildfires and the influence of absorbing and non-absorbing organic coatings on spectral light absorption. *Atmospheric Chemistry and Physics* **2009**, *9*, 8007–8015.

(4) Niemi, J. V.; Tervahattu, H.; Vehkamäki, H.; Martikainen, J.; Laakso, L.; Kulmala, M.; Aarnio, P.; Koskentalo, T.; Sillanpää, M.; Makkonen, U. Characterization of aerosol particle episodes in Finland caused by wildfires in Eastern Europe. *Atmospheric Chemistry and Physics Discussions* **2005**, *5*, 2469–2501.

(5) Guazzotti, S. A.; Suess, D. T.; Coffee, K. R.; Quinn, P. K.; Bates, T. S.; Wisthaler, A.; Hansel, A.; Ball, W. P.; Dickerson, R. R.; Neusüß, C.; et al., Characterization of carbonaceous aerosols outflow from India and Arabia: Biomass/biofuel burning and fossil fuel combustion. *Journal of Geophysical Research: Atmospheres* **2003**, *108*, 13.

(6) Gustafsson, ; Kruså, M.; Zencak, Z.; Sheesley, R. J.; Granat, L.; Engström, E.; Praveen, P. S.; Rao, P. S. P.; Leck, C.; Rodhe, H. Brown Clouds over South Asia: Biomass or Fossil Fuel Combustion? *Science* **2009**, *323*, 495–498.

(7) Yan, C.; Zheng, M.; Shen, G.; Cheng, Y.; Ma, S.; Sun, J.; Cui, M.; Zhang, F.; Han, Y.; Chen, Y. Characterization of carbon fractions in carbonaceous aerosols from typical fossil fuel combustion sources. *Fuel* **2019**, *254*, 115620.

(8) Roberts, D. L.; Jones, A. Climate sensitivity to black carbon aerosol from fossil fuel combustion. *Journal of Geophysical Research: Atmospheres* **2004**, *109*, D16202.

(9) Chen, G.; Feng, Q.; Wang, J. Mini-review of microplastics in the atmosphere and their risks to humans. *Science of The Total Environment* **2020**, *703*, 135504.

(10) Zhang, Y.; Gao, T.; Kang, S.; Sillanpää, M. Importance of atmospheric transport for microplastics deposited in remote areas. *Environmental Pollution* **2019**, *254*, 112953.

(11) Dris, R.; Gasperi, J.; Saad, M.; Mirande, C.; Tassin, B. Synthetic fibers in atmospheric fallout: A source of microplastics in the environment? *Marine Pollution Bulletin* **2016**, *104*, 290–293.

(12) Zhang, Y.; Kang, S.; Allen, S.; Allen, D.; Gao, T.; Sillanpää, M. Atmospheric microplastics: A review on current status and perspectives. *Earth-Science Reviews* **2020**, *203*, 103118.

(13) Obbard, R. W. Microplastics in Polar Regions: The role of long range transport. *Current Opinion in Environmental Science & Health* **2018**, *1*, 24–29.

(14) Bergmann, M.; Mützel, S.; Primpke, S.; Tekman, M. B.; Trachsel, J.; Gerdts, G. White and wonderful? Microplastics prevail in snow from the Alps to the Arctic. *Science Advances* **2019**, *5*, eaax1157.

(15) Allen, S.; Allen, D.; Phoenix, V. R.; Le Roux, G.; Durántez Jiménez, P.; Simonneau, A.; Binet, S.; Galop, D. Atmospheric transport and deposition of microplastics in a remote mountain catchment. *Nature Geoscience* **2019**, *12*, 339–344.

(16) Sloane, C. S.; Rood, M. J.; Rogers, C. F. Measurements of Aerosol Particle Size: Improved Precision by Simultaneous Use of Optical Particle Counter and Nephelometer. *Aerosol Science and Technology* **1991**, *14*, 289–301.

(17) Leong, K. H.; Jones, M. R.; Holdridge, D. J.; Ivey, M. Design and Test of a Polar Nephelometer. *Aerosol Science and Technology* **1995**, *23*, 341–356.

(18) Dolgos, G.; Martins, J. V. Polarized Imaging Nephelometer for in situ airborne measurements of aerosol light scattering. *Opt. Express, OE* **2014**, *22*, 21972–21990.

(19) Manfred, K. M.; Washenfelder, R. A.; Wagner, N. L.; Adler, G.; Erdesz, F.; Womack, C. C.; Lamb, K. D.; Schwarz, J. P.; Franchin, A.; Selimovic, V.; et al., Investigating biomass burning aerosol morphology using a laser imaging nephelometer. *Atmospheric Chemistry and Physics* **2018**, *18*, 1879–1894.

(20) Abo Riziq, A.; Erlick, C.; Dinar, E.; Rudich, Y. Optical properties of absorbing and non-absorbing aerosols retrieved by cavity ring down (CRD) spectroscopy. *Atmospheric Chemistry and Physics* **2007**, *7*, 1523–1536.

(21) Toole, J. R.; Renbaum-Wolff, L.; Smith, G. D. A Calibration Technique for Improving Refractive Index Retrieval from Aerosol Cavity Ring-Down Spectroscopy. *Aerosol Science and Technology* **2013**, *47*, 955–965.

(22) Nakayama, T.; Hagino, R.; Matsumi, Y.; Sakamoto, Y.; Kawasaki, M.; Yamazaki, A.; Uchiyama, A.; Kudo, R.; Moteki, N.; Kondo, Y.; et al., Measurements of aerosol optical properties in central Tokyo during summertime using cavity ring-down spectroscopy: Comparison with conventional techniques. *Atmospheric Environment* **2010**, *44*, 3034–3042.

(23) Miles, R. E. H.; Rudić, S.; Orr-Ewing, A. J.; Reid, J. P. Influence of Uncertainties in the Diameter and Refractive Index of Calibration Polystyrene Beads on the Retrieval of Aerosol Optical Properties Using Cavity Ring Down Spectroscopy. *J. Phys. Chem. A* **2010**, *114*, 7077–7084.

(24) Ogieglo, W.; Wormeester, H.; Eichhorn, K.-J.; Wessling, M.; Benes, N. E. In situ ellipsometry studies on swelling of thin polymer films: A review. *Progress in Polymer Science* **2015**, *42*, 42–78.

(25) Wu, C.; Xia, K.-Q. Incorporation of a differential refractometer into a laser light-scattering spectrometer. *Review of Scientific Instruments* **1998**, *65*, 587.

(26) Beaucage, G.; Composto, R.; Stein, R. S. Ellipsometric study of the glass transition and thermal expansion coefficients of thin polymer films. *Journal of Polymer Science Part B: Polymer Physics* **1993**, *31*, 319–326.

(27) Krause, S.; Lu, Z.-H. Refractive index–temperature measurements on anionically polymerized polystyrene. *Journal of Polymer Science: Polymer Physics Edition* **1981**, *19*, 1925–1928.

(28) Efremov, M. Y.; Soofi, S. S.; Kiyanova, A. V.; Munoz, C. J.; Burgardt, P.; Cerrina, F.; Nealey, P. F. Vacuum ellipsometry as a method for probing glass transition in thin polymer films. *Review of Scientific Instruments* **2008**, *79*, 043903.

(29) He, J.; Liu, W.; Huang, Y.-X. Simultaneous Determination of Glass Transition Temperatures of Several Polymers. *PLOS ONE* **2016**, *11*, e0151454.

(30) Hutchinson, J. M. Determination of the glass transition temperature. *J Therm Anal Calorim* **2009**, *98*, 579.

(31) Ashkin, A.; Dziedzic, J. M.; Yamane, T. Optical trapping and manipulation of single cells using infrared laser beams. *Nature* **1987**, *330*, 769.

(32) Jones, S. H.; King, M. D.; Ward, A. D. Determining the unique refractive index properties of solid polystyrene aerosol using broadband Mie scattering from optically trapped beads. *Physical Chemistry Chemical Physics* **2013**, *15*, 20735–20741.

(33) Wills, J. B.; Knox, K. J.; Reid, J. P. Optical control and characterisation of aerosol. *Chemical Physics Letters* **2009**, *481*, 153–165.

(34) Ashkin, A. Optical trapping and manipulation of neutral particles using lasers. *Proceedings of the National Academy of Sciences* **1997**, *94*, 4853–4860.

(35) Ashkin, A.; Dziedzic, J. M.; Bjorkholm, J. E.; Chu, S. Observation of a single-beam gradient force optical trap for dielectric particles. *Optics Letters* **1986**, *11*, 288–290.

(36) Preston, T. C.; Mason, B. J.; Reid, J. P.; Luckhaus, D.; Signorell, R. Size-dependent position of a single aerosol droplet in a Bessel beam trap. *Journal of Optics* **2014**, *16*, 025702.

(37) Thanopulos, I.; Luckhaus, D.; Preston, T. C.; Signorell, R. Dynamics of submicron aerosol droplets in a robust optical trap formed by multiple Bessel beams. *Journal of Applied Physics* **2014**, *115*, 154304.

(38) David, G.; Esat, K.; Hartweg, S.; Cremer, J.; Chasovskikh, E.; Signorell, R. Stability of aerosol droplets in Bessel beam optical traps under constant and pulsed external forces. *The Journal of Chemical Physics* **2015**, *142*, 154506.

(39) Li, T. *Fundamental Tests of Physics with Optically Trapped Microspheres*; Springer Science & Business Media, 2012.

(40) Brandrup, J., Immergut, E. H., Grulke, E. A., Eds. *Polymer handbook*, 4th ed.; Wiley: New York, 1999.

(41) Rieger, J. The glass transition temperature of polystyrene. *Journal of thermal analysis* **1996**, *46*, 965–972.

(42) Richardson, M. J.; Savill, N. G. Derivation of accurate glass transition temperatures by differential scanning calorimetry. *Polymer* **1975**, *16*, 753–757.

(43) Aras, L.; Richardson, M. J. The glass transition behaviour and thermodynamic properties of amorphous polystyrene. *Polymer* **1989**, *30*, 2246–2252.

(44) Wunderlich, B.; Bodily, D. M.; Kaplan, M. H. Theory and Measurements of the Glass-Transformation Interval of Polystyrene. *Journal of Applied Physics* **1964**, *35*, 95–102.

(45) Jenkins, F. A.; White, H. E. *Fundamentals of optics*; Mc Graw-Hill Primis Custom Publ.: New York, 2010.

(46) Jones, S. H.; King, M. D.; Ward, A. D. Atmospherically relevant core–shell aerosol studied using optical trapping and Mie scattering. *Chemical Communications* **2015**, *51*, 4914–4917.

(47) Lew, L. J. N.; Ting, M. V.; Preston, T. C. Determining the size and refractive index of homogeneous spherical aerosol particles using Mie resonance spectroscopy. *Applied Optics* **2018**, *57*, 4601–4609.

(48) Conwell, P. R.; Rushforth, C. K.; Benner, R. E.; Hill, S. C. Efficient automated algorithm for the sizing of dielectric microspheres using the resonance spectrum. *JOSA A* **1984**, *1*, 1181–1187.

(49) David, G.; Esat, K.; Ritsch, I.; Signorell, R. Ultraviolet broadband light scattering for optically-trapped submicron-sized aerosol particles. *Physical Chemistry Chemical Physics* **2016**, *18*, 5477–5485.

(50) Schmitz, M.; Rothe, T.; Kienle, A. Evaluation of a spectrally resolved scattering microscope. *Biomedical Optics Express* **2011**, *2*, 2665–2678.

(51) Bohren, C. F.; Huffman, D. R. *Absorption and Scattering of Light by Small Particles*; John Wiley & Sons, Ltd, 2007; pp 82–129.

(52) Huckaby, J. L.; Ray, A. K.; Das, B. Determination of size, refractive index, and dispersion of single droplets from wavelength-dependent scattering spectra. *Applied Optics* **1994**, *33*, 7112–7125.

(53) Lorentz H. A., *The theory of electrons*; Leipzig: B. G. Teubner: New York, 1916.

(54) Fiaz, M.; Beevers, M. S. Temperature dependence of static dielectric permittivity and dipole moments of poly(N-vinylcarbazole). *Polymer* **1996**, *37*, 755–760.

(55) Priyadarshi, A.; Shimin, L.; Mhaisalkar, S. G.; Rajoo, R.; Wong, E. H.; Kripesh, V.; Namdas, E. B. Characterization of optical properties of acrylate based adhesives exposed to different temperature conditions. *Journal of Applied Polymer Science* **2005**, *98*, 950–956.

(56) Liu, Y.; Daum, P. H. Relationship of refractive index to mass density and self-consistency of mixing rules for multicomponent mixtures like ambient aerosols. *Journal of Aerosol Science* **2008**, *39*, 974–986.

(57) Tan, C.-Y.; Huang, Y.-X. Dependence of Refractive Index on Concentration and Temperature in Electrolyte Solution, Polar Solution, Nonpolar Solution, and Protein Solution. *Journal of Chemical & Engineering Data* **2015**, *60*, 2827–2833.

(58) Ciddor, P. E. Refractive index of air: new equations for the visible and near infrared. *Applied Optics* **1996**, *35*, 1566–1573.